Available online at www.sciencedirect.com
SCIENCE DIRECT®

ELSEVIER

Journal of Catalysis 232 (2005) 342–354

JOURNAL OF CATALYSIS

www.elsevier.com/locate/jcat

Optimizing the conversion of heavy reformate streams into xylenes with zeolite catalysts by using knowledge base high-throughput experimentation techniques

José M. Serra [a], Emmanuelle Guillon [b], Avelino Corma [a,*]

[a] *Instituto de Tecnología Química, UPV-CSIC, Av. de los Naranjos s/n, 46022 Valencia, Spain*
[b] *Institut Français du Pétrole, CEDI René Navarre, BP 3, 69390 Vernaison, France*

Received 27 December 2004; revised 8 March 2005; accepted 14 March 2005

Abstract

The conversion of commercial heavy reformates under industrially relevant transalkylation conditions was studied over seven different acid zeolite catalysts with channel systems containing 10 MR, 12 MR, and 10 + 12 MR pores, by high-throughput experimentation (HTE). Zeolites were impregnated with seven different metals (Re, Pt, Mo, Ga, Ni, La, Bi). The reaction network for the global process was established, and the initial rates for primary reactions were estimated. It was found that zeolite pore size and geometry have a direct influence on dealkylation and transalkylation of the different alkyl groups. The ethyl and propyl dealkylation rate increases, while the rate of alkyl group transalkylation decreases as the zeolite pore dimensions decrease. A multizeolitic catalyst has been designed to optimize the dealkylation of ethyl and propyl aromatics while producing the transalkylation of tri- and tetramethylbenzene with toluene/benzene in order to maximize xylene yield when during the processing of heavy reformate.

Keywords: Xylenes; Transalkylation; Dealkylation; Zeolites; Heavy reformate; HTE

---

1. Introduction

A very high range of consumer products, from solvents to fibers, films, and plastics, are based on BTX. Xylenes, especially the *para*-xylene isomer, are in great demand for the manufacture of polyester monomers like terephthalic acid and dimethylterephthalate. BTX is produced by naphtha reforming and pyrolysis, in which the proportion of each aromatic is controlled thermodynamically. Therefore, there is a substantial mismatch between the market supply and demand [1] for the different aromatics; that is, valuable xylenes are produced in lower amounts, whereas toluene, for which the demand is low, is always produced in surplus.

In a typical aromatics complex process based on catalytic reforming, toluene and heavy reformate are catalytically converted in two different units with the aim of maximizing xylene production. On the one hand, the disproportionation unit typically uses toluene as feed and preferentially produces benzene and xylenes in similar proportions, permitting the selective production of p-xylene. On the other hand, the transalkylation unit treats feedstreams comprising mixtures of toluene/benzene and heavy reformate (A_{10}^+) in different proportions and produces principally xylenes and, in lower amounts, benzene and LPGs.

Transalkylation of methyl-aromatics to yield xylenes is carried out over bifunctional zeolitic catalysts under hydrogen pressure. Nickel impregnated with mordenite or exchanged over dealuminated mordenite is the most popular catalyst and is used, for example, in the Tatoray [2,3] and TransPlus [4] commercial processes. However, Ni–mordenite catalyst suffers from catalyst deactivation by coking and gives low conversion of ethyl- and propyl-aromatics contained in heavy reformate. A tailor-made transalkylation

---

[*] Corresponding author. Fax: +34 96 3877809.
E-mail address: acorma@itq.upv.es (A. Corma).

0021-9517/$ – see front matter © 2005 Elsevier Inc. All rights reserved.
doi:10.1016/j.jcat.2005.03.021

Table 1
Metals used in zeolitic catalysts for different alkyl-aromatics conversion processes

Metal	wt%	Zeolite	Method	Feed	H_2/HC	Pressure (bar)	Temperature (°C)	WHSV (h^{-1})	Reference
Pt	0.2	BEA	Incipient wetness	$A_9^+ + \mathrm{Tol}$	6	25	460	2.6	[29]
Pd	0.3	MOR	Ion exchange	$A_9^+ + \mathrm{Tol}$	2–5	13.6–27.2	290–425	1.4–4	[30]
Ni	1	MAZ	Ion exchange	$A_9^+ + \mathrm{Tol}$	3–12	20–45	330–500	0.5–4	[31–33]
Re	0.15	MOR	Incipient wetness	$A_9^+ + \mathrm{Tol}$	3–12	20–45	330–500	0.5–4	[34–36]
La	4	BEA	Incipient wetness	$A_9^+ + \mathrm{Tol}$	–	17–51	400–650	0.1–30	[37]
Mo	2	BEA	Incipient wetness	$A_9^+ + \mathrm{Tol}$	–	17–51	400–650	0.1–30	[37]
La + Mo	3.8/3	BEA	Incipient wetness	$A_9^+ + \mathrm{Tol}$	–	17–51	400–650	0.1–30	[38]
Ga, Bi	1	MFI	Incipient wetness	$A_9^+ + \mathrm{Tol}$	0.25–5	3.4–34	400–500	1–10	[39]
Ag, Bi, Cu, Pb	0.1–1	MOR	Incipient wetness	$A_9^+ + \mathrm{Tol}$	2–10	15–40	300–600	0.5–3	[40]
Cr, W, Co	0.2	MOR	Incipient wetness	A_9^+	4	10–60	300–550	0.1–10	[41]

catalyst would be intended to (a) improve the global catalytic activity, permitting an increase in heavy reformate conversion and xylenes production with the same facilities; (b) increase the selectivity of the process by reducing the final concentration of by-products like naphthenes, ethylbenzene, light products from cracking, and heavy alkyl-aromatics; and (c) increase catalyst life, thus prolonging regeneration cycles. Targets (a) and (b) can be achieved by maximization of the dealkylation activity of ethyl- and propyl-aromatics and by balancing of the hydrogenation function of the metal component, and target (c) can be achieved by cessation of the formation of heavy aromatics that block the pore system and by rapid hydrogenation of the olefins produced by dealkylation and cracking.

As stated previously [5], zeolite topology plays an important role on the activity of the different dealkylation and transalkylation reactions involved in the general reaction scheme of the process. In addition, channel connectivity and dimensions could restrict the formation of bulky transition states [6–8], influencing the deactivation/coking mechanisms and kinetics. Furthermore, the addition of hydrogenating metals to the zeolites increases the catalyst life, but it could also influence the selectivity of the transalkylation/dealkylation process. Tsai et al. [9] have discussed the convenience of developing a metallic function that selectively hydrogenates polyaromatics (naphthalenes [10,11]), which are coke precursors, while minimizing benzene hydrogenation. We show in Table 1 a summary of different metals (Cu, Ni, Pt, Re, Pd, etc.) that can be used in the transalkylation and/or dealkylation of alkylaromatics.

In the present work, we studied the dealkylation-transalkylation performance of different metal/zeolite catalysts with high-throughput experimentation (HTE) techniques. A new catalyst system has been developed that improves the existing results for heavy reformate processing to maximize xylene production.

1.1. Thermodynamic study

Since heavy reformate transalkylation is a thermodynamically controlled process, the final yield of xylenes and benzene is limited by the reactor feed composition. Considering the composition of the industrial feed employed here, we can calculate (Fig. 1) the equilibrium composition as a function of the ratio of toluene to heavy reformate in feed. For this calculation, we have made the following approximations: only dealkylation and transalkylation reactions are occurring, and alkene and aromatic ring hydrogenation, nonselective cracking, dealkylation of methyl groups, and formation of polyaromatics like naphthalene or anthracene derivatives are not occurring.

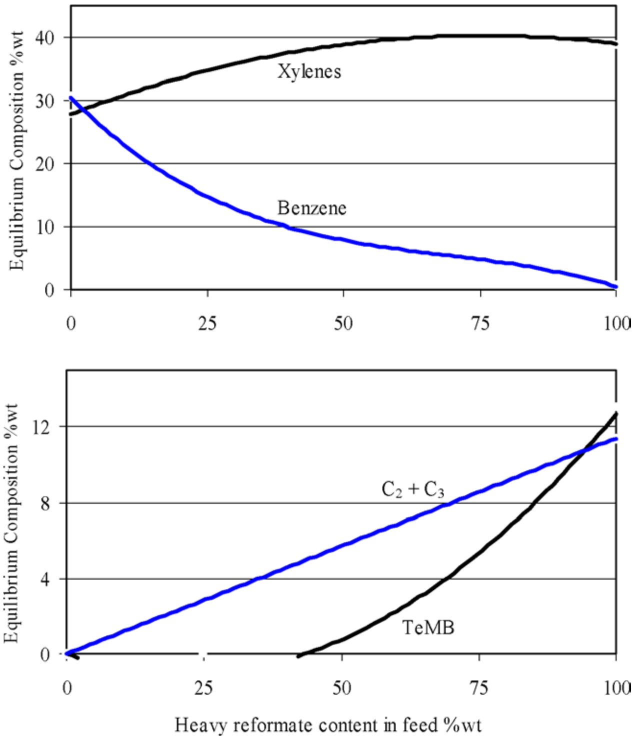

Fig. 1. Equilibrium composition of transalkylation products as a function of the content of heavy reformate in feed (mixed with toluene).

These results show that ethyl- and propyl-aromatics can be fully dealkylated, producing benzene, toluene, xylenes, and olefins as primary products. The yield of xylenes is thermodynamically controlled. For instance, for a reformate content of 50 wt% and 50% toluene, the xylene yield is 38 wt%, and trimethylbenzene (TMB) conversion is about 64%, whereas the benzene and tetramethylbenzene (TeMB) yields are 8.8 and 0.5%, respectively. The maximum yield of xylenes is achieved at ∼ 75 wt% reformate and 25% toluene. However, in this situation the TeMB yield at equilibrium is as much as ∼ 5%. Therefore, from a thermodynamic point of view, the optimum reformate content is about 50%, since the ratio of xylenes to TeMB in the products is maximized.

2. Experimental

2.1. Reactants

Heavy reformate composition is given in Table 2. Toluene (99.9%) was supplied by Scharlau, and H_2 (99.99%) was supplied by Linde.

Table 2
Composition of the commercial heavy reformate employed in the catalytic testing

A_8	*m*-, *p*-Xylene	0.00		
	o-Xylene	0.33		
A_9	*i*-Propylbenzene	1.64	C_3-Bz	5.6
	n-Propylbenzene	4.01		
	1,3,5-Trimethylbenzene	8.55	TMB	54.5
	1,2,4-Trimethylbenzene	38.5		
	1,2,3-Trimethylbenzene	7.39		
	1-Methyl-3-ethylbenzene	18.5	ET	32.9
	1-Methyl-4-ethylbenzene	7.39		
	1-Methyl-2-ethylbenzene	6.54		
	Indane	0.41		
	Indene	0.22		
A_{10}	1-Methyl-3-isopropylbenzene	0.44		
	1,3-Diethylbenzene	1.46		
	1-Methyl-3-*n*-propylbenzene	1.34		
	1,4-Dimethyl-2-ethylbenzene	0.38	EX	2.79
	1,3-Dimethyl-4-ethylbenzene	0.41		
	1,2-Dimethyl-4-ethylbenzene	1.85		
	1,3-Dimethyl-2-rthylbenzene	0.04		
	1,2-Dimethyl-3-ethylbenzene	0.12		
	1,2,4,5-Tetramethylbenzene	0.12	TeMB	0.25
	1,2,3,5-Tetramethylbenzene	0.13		
	1-Methylindane	0.05		
$A_{11}{}^{+}$	Aromatics with more than ten C	0.02		

2.2. Catalyst preparation

Y, Beta, mordenite, and ZSM-5 zeolites were commercial samples supplied by PQ (CBV7020, CP811, CBV30A, and CBV3020 products). Zeolite NU-87, IM-5, and ITQ-23 were synthesized in our laboratory with the procedures reported in [12–15]. Na-zeolites were converted into the acid form by ion exchange with ammonium chloride for 2 h at 80 °C and ulterior calcination at 580 °C for 5 h. Table 3 gives a summary of the characteristics of H-zeolites. The structure of IM-5 is not known, though it has been suggested [13] that it could have a pore topology formed by either 10 MR crossing pores or 10 MR pores with lobes, and the pore diameter should be close to but somewhat smaller than 5.5 Å. NU-87 (NES structure) contains 12-MR cages with four 10-MR entrances forming channels [12]. Finally, ITQ-23 (CON structure) has a three-dimensional pore system formed by 10- and 12-MR pores [15].

The acid samples were impregnated with an aqueous solution of corresponding metal precursor: $HReO_4$ (Acros Organics, 76.5%), $H_2PtCl_6 \cdot 4.5H_2O$ (Aldrich, 99.9%), $(NH_4)_6Mo_7O_{24} \cdot 4H_2O$ (Merck, 99%), $Ni(NO_3)_3 \cdot 6H_2O$ (Fluka, 99%), $Ga(NO_3)_3 \cdot 10H_2O$ (Strem Chem, 99.99%), $Bi(NO_3)_3 \cdot 5H_2O$ (Merck, 99%), $La(NO_3)_3 \cdot 6H_2O$ (Merck, 99%). Thus, all of the metals were incorporated to the zeolitic catalyst by impregnation. After that, the samples were dried at 100 °C overnight, calcined at 500 °C for 2 h, and pelleted. Finally, they were reduced in hydrogen flow at 450 °C for 1 h in the catalytic testing rig. In the case of zeolite mixtures, the impregnated and calcined samples were mixed and milled together before pelleting.

2.3. Characterization

A Nicolet 710 FTIR spectrometer was used to follow the pyridine adsorbed to the acid sites of the acid zeolites calcined at 500 °C for 2 h. To do this, self-supported wafers with 10 mg/cm^2 were pretreated overnight under vacuum at 400 °C and cooled to room temperature. After acquisition of the spectrum in the OH stretching region, pyridine vapor (6.6 kPa) was admitted to the cell until equilibrium was reached. The samples were then desorbed under vacuum (10^{-3} mbar)

Table 3
Composition and physico-chemical characterization of zeolitic samples

Zeolite	Code	Channels	Si/Al	Pore Volume (cm^3/g)	Acidity ($\mu mol_{pyr}/g$)			
					Brönsted		Lewis	
					250 °C [a]	350 °C [a]	250 °C [a]	350 °C [a]
ZSM-5	MFI	10 × 10 MR	18	0.12	44	25	9	6
IM-5	–	10 × 10 MR	15	0.13	29	17	7	6
Mordenite	MOR	12 MR	18	0.15	79	37	25	24
NU-87	NES	10 × 12 MR	16	0.16	70	48	26	24
ITQ-23	–	10 × 12 × 12 MR	15	0.18	49	29	37	31
Beta	BEA	12 × 12 MR	13	0.20	31	15	53	42
Y	FAU	12 × 12 MR	14	0.233	59	31	9	8

[a] Pyridine desorption temperature.

at 250 and 350 °C with spectra acquisition at room temperature after each desorption treatment. All of the spectra were scaled according to the sample weight. Absorption coefficients calculated by Emeis [16] were used. The pore volume and microporous surface area of the samples were obtained with an ASAP 2000 apparatus. Calculations were performed by the method developed by De Boer et al. [17], with the use of the N_2 absorption isotherms at 77 K.

2.4. Catalytic studies

Catalytic work was carried out with a system [18,19] of 16 continuous fixed-bed parallel microreactors (Spider reactor). Each reactor is fed and the flow controlled and measured independently in each reactor, making it possible to operate in a wide range of contact times and hydrogen/hydrocarbon ratios. The liquid feed was composed of 50 wt% commercial heavy reformate (Table 2) and 50 wt% toluene. The reproducibility of the system was checked against a reference catalyst supplied by IFP (Ni/mordenite/γ-Al_2O_3), which was introduced into one reactor as the standard in each round of experiments.

The simultaneous catalytic experiments were carried out under the following conditions: 25 bar total pressure, 400 °C, hydrogen/hydrocarbon ratio of 8.5 mol mol^{-1}, reaction time longer than 8 h, and the WHSV was varied from 0.8 to 800 h^{-1}. The amount of catalyst (particle size 0.4–0.6 mm) in each fixed-bed microreactor was 200 mg. Reaction products were analyzed on line with a gas chromatograph (Varian 3800GC) equipped with a diphenyldimethylpolysiloxane capillary column. Conversion (X, %) of feed constituents and yield (Y, %) of the different reaction products were calculated with regard to their corresponding concentration (wt%) in the feed or in the reaction products

$$\text{Conversion of A} = \big(\big([\text{A}]_{\text{Feed}} - [\text{A}]_{\text{Products}}\big) \times 100\big)/[\text{A}]_{\text{Feed}},$$

$$\text{Yield of B} = [\text{B}]_{\text{Products}}.$$

3. Results and discussion

3.1. Reaction network

To establish the primary and secondary reactions that occur when heavy reformate is processed, the yields of the different products were obtained at different levels of conversion. We did this by reacting the commercial reformate mixed with toluene at different space velocities (0.8–800 h^{-1}) and using zeolite beta impregnated with 0.3 wt% rhenium (Re/beta) as a catalyst (Fig. 2).

The results obtained at very short contact times (Table 4) show that transalkylation products like the nondesired heavy aromatics (A_{11}^{+}), EB, or TeMB are formed preferentially in the first part of the catalytic bed, whereas ethane is formed only by dealkylation in very small amounts (0.01 wt% at WHSV 800 h^{-1}). Therefore, the initial rate for transalkylation of methyl, ethyl, and propyl groups should be higher than the rate for dealkylation. This is particularly true for ethyl groups. These results are in agreement with the former studies on dealkylation/transalkylation with model reactants such as ethylbenzene and ethyltoluene [5].

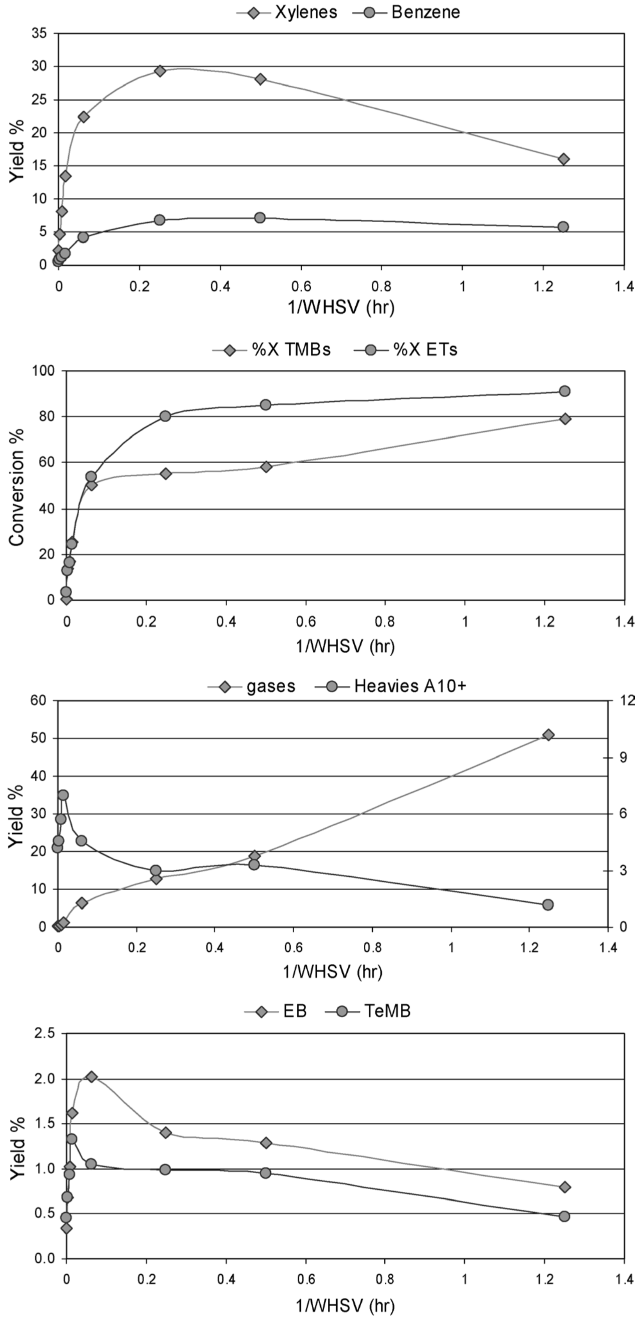

Fig. 2. Evolution of catalytic performance for Re/beta catalysts for a wide WHSV range (400 °C, $H_2/HC = 8.5$, and TOS ≈ 8 h).

When the contact time is increased (up to WHSV ≈ 4 h^{-1}), the yield of benzene and xylenes increases and the yield of unstable aromatics like EB and A_{11}^{+} is progressively reduced by dealkylation of the alkyl groups (Fig. 2). At higher contact times (WHSV lower than 3 h^{-1}), the

Table 4
Catalytic performance of Re/beta catalyst for short contact times (400 °C, $H_2/HC = 8.5$, and TOS ≈ 8 h; X (%) conversion and Y (wt%) yield)

	WHSV (h^{-1})			
	800	400	128	64
Xylenes Y	2.3	4.7	8.1	13.5
Benzene Y	0.5	0.8	1.2	1.7
TMB X	2.6	14.0	17.1	25.4
Thane Y	0.01	0.04	0.06	0.12
EB Y	0.3	0.7	1.0	1.6
ET X	3.5	13.1	16.7	24.2
EX X	−9.0	−13.8	−28.3	−51.3
A_{10} Y	3.7	3.7	4.4	5.2
A_{11}^{+} Y	0.47	0.80	1.26	1.75
$C_1 + C_4^{+}$ Y	0.22	0.40	0.63	1.15

Table 5
Summary of the main formation reactions of the principal products observed in the conversion of heavy reformate mixed with toluene

Xylenes formation
$\text{Tol} + \text{Tol} \rightarrow \text{Bz} + \text{Xyl}$
$\text{Tol} + \text{TMB} \rightarrow \text{Xyl} + \text{Xyl}$
$\text{ET} + \text{Tol} \rightarrow \text{Xyl} + \text{EB}$
$\text{EX} \rightarrow \text{Xyl} + C_2$
$\text{TMB} + \text{TMB} \rightarrow \text{TeMB} + \text{Xyl}$

Benzene formation
$\text{Tol} + \text{Tol} \rightarrow \text{Bz} + \text{Xyl}$
$C_3\text{-Bz} \rightarrow \text{Bz} + C_3$
$\text{Tol} + \text{TMB} \rightarrow \text{Bz} + \text{TeMB}$

Toluene formation
$\text{ET} \rightarrow \text{Tol} + C_2$
$\text{ET} + \text{ET} \rightarrow \text{Tol} + A_{11}$
$C_3\text{-Bz} \rightarrow \text{Tol} + C_2$
$C_3\text{-Bz} + \text{Tol} \rightarrow \text{ET} + \text{Tol}$

Ethylbenzene formation
$\text{ET} + \text{Tol} \rightarrow \text{EB} + \text{Xyl}$
$\text{ET} + \text{ET} \rightarrow \text{EB} + \text{EX}$

Heavy products (A_{10}^{+}) formation
$\text{Tol} + \text{ET} \rightarrow \text{Bz} + A_{10}$
$\text{ET} + \text{ET} \rightarrow \text{Tol} + A_{11}$
$\text{ET} + \text{ET} \rightarrow \text{EB} + A_{10}$
$\text{Tol} + \text{TMB} \rightarrow \text{Bz} + A_{10}$
$\text{TMB} + \text{TMB} \rightarrow \text{Xyl} + A_{10}$
$\text{ET} + \text{TMB} \rightarrow \text{Tol} + A_{11}$
$C_3\text{-Bz} + \text{Tol} \rightarrow \text{Bz} + A_{10}$
⋮

yield of cracking reactions increases, producing principally ethane, propane, and butanes, and reducing a final yield of aromatic compounds, specially toluene, xylenes, and benzene. As a result, equilibrium composition (Fig. 1) is never reached, because of the nonselective cracking reaction.

Taking into account the reaction network established for transalkylation/dealkylation of heavy reformate and pure ethylaromatics [5], the expected reactions occurring during the transalkylation of heavy reformate are summarized in Table 5, where primary reactions are classified, with the principal reaction products taken into account.

3.2. *Influence of zeolite structure on product distribution*

Catalytic results at 400 °C and WHSV ≈ 4 h^{-1} for the different zeolites impregnated with rhenium (0.3 wt%) are given in Fig. 3. The results include conversion of toluene and heavy reformate products and yield of xylenes, benzene, and nondesired reaction products.

It can be seen there that medium pore zeolites (ZSM-5 and IM-5) are the most active structures for the dealkylation of ethyltoluene to form toluene and ethylene, which is totally hydrogenated to ethane. The general trend observed in the ethyltoluene conversion is that the larger the pore size of the zeolite, the lower the dealkylation activity is (Figs. 3C–D). Thus, dealkylation is favored over transalkylation when the degree of confinement of the ET molecule inside the zeolite pore system is increased, which increases the geometrical restrictions to the formation of bulkier bimolecular transition states that lead to transalkylation. This behavior can be further confirmed by observing (Fig. 3F) the conversion of other alkyl-aromatics from reformate, such as ethylxylenes (EX) and propyl-benzenes (C_3-Bz). Furthermore, it can also be concluded that isopropyl dealkylation is faster than n-propyl dealkylation, because of the formation of more stable secondary cation on the dealkylated propyl group in isopropyl and the fact that n-propylbenzene transalkylates faster than cumene.

In the case of trimethylbenzene (TMB) conversion (Fig. 3D), which involves methyl transalkylation reactions, the highest TMB conversion is achieved with tridirectional large-pore zeolites like beta or Y. TMB diffusion and the formation of the bimolecular transition states required for transalkylation of the methyl group from TMB to toluene is favored inside the large pores. Disproportionation of two molecules of TMB produces one molecule of xylene and another of tetramethylbenzene (TeMB), which is the last product detected in similar amounts regardless of the zeolite catalyst (Fig. 3E), indicating that this reaction should mainly occur on the external surface of the zeolite crystallites.

Toluene is produced and consumed through different reactions (Table 5), such as conversion through transalkylation with TMB, formation through ET dealkylation, etc. Therefore, toluene conversion is higher for large-pore zeolites like Y or beta with high transalkylation activity and low dealkylation degree, whereas toluene formation is favored in medium-pore zeolites such as ZSM-5 (Fig. 3F).

The yields of xylenes and benzene make it possible to evaluate the catalyst activity for transalkylation of methyl groups and dealkylation of reformate molecules (ET and EX). Table 5 shows the main reactions involved in the formation of xylenes, which are the most important factor in the transalkylation of toluene and TMB (principal constituents of the feed). The lowest yield of xylenes (Fig. 3A) is obtained with medium- and large-pore zeolites, and the highest xylene yield was obtained with zeolites containing a combination of 10 MR and 12 MR or 8 MR and 12MR, like NU-87 or mordenite, respectively. In fact, the best-performing structures combine a high deethylation activity with a high transmethylation activity (see Fig. 4). Xylene isomer distribution was that corresponding to the thermodynamic equilibrium (24/53/24 = *para*/*meta*/*ortho*) for all of the tested zeolites.

Benzene is formed principally through the disproportionation of toluene and dealkylation of propyl-benzenes. To a smaller extent, benzene can also be formed through transalkylation of the methyl group of toluene to an A_9 molecule (TMB or ET), yielding heavy products (A_{10}) over acid sites located on large intrazeolitic cages or at the external

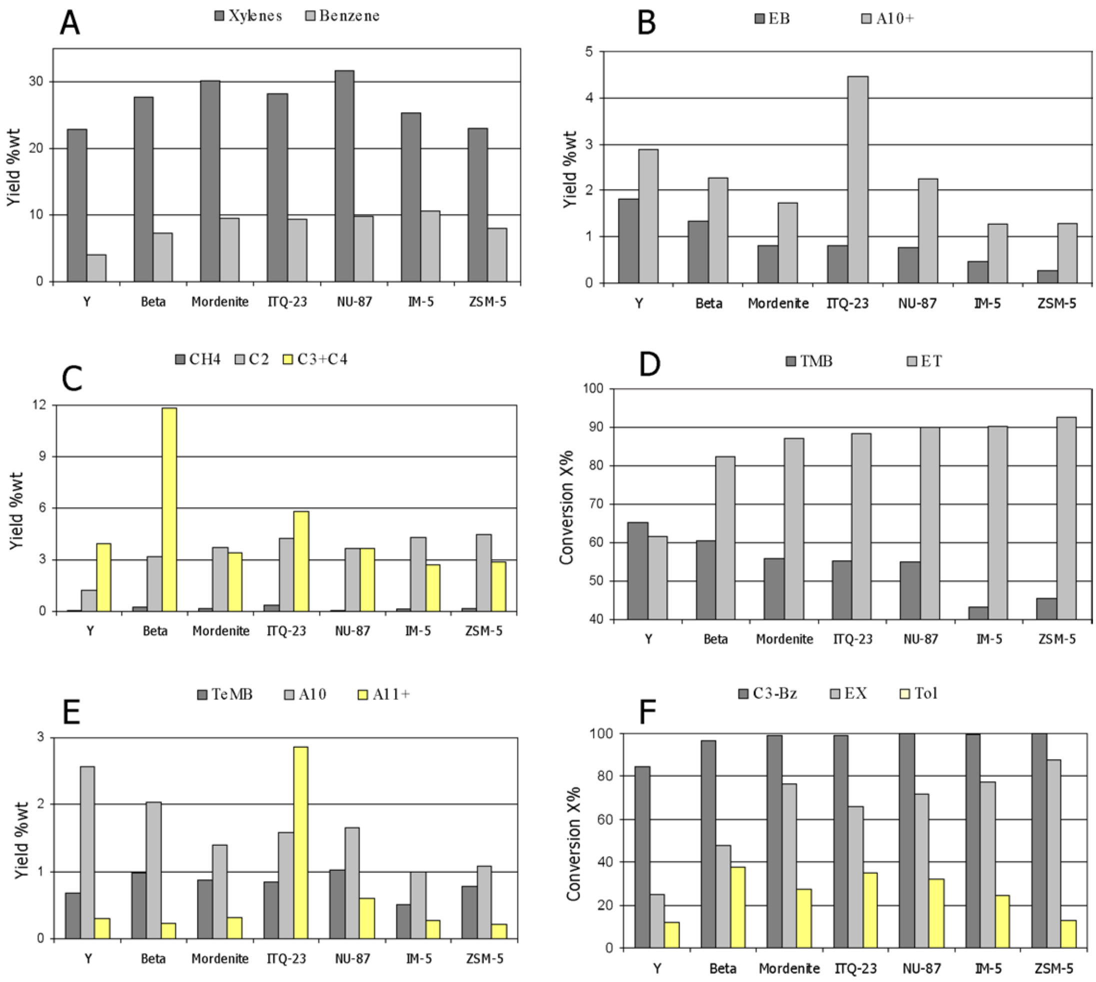

Fig. 3. Influence of the zeolite structure (Re 0.3%) on the catalytic conversion of heavy reformate (400 °C, WHSV = 4 h^{-1}, $H_2/HC = 8.5$, and TOS ≈ 8 h).

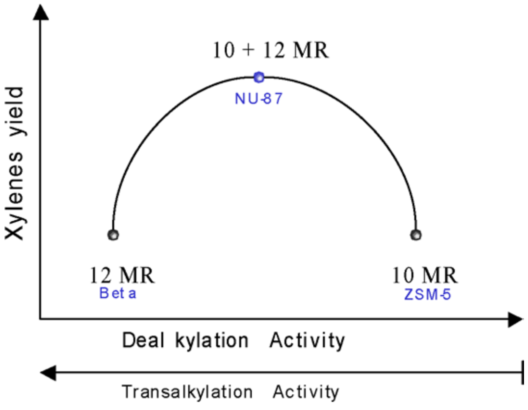

Fig. 4. Dependence of xylenes yield on zeolite topology.

zeolite surface. The highest benzene yield is obtained with medium-pore zeolites (ZSM-5 and IM-5) and mordenite, and, with these zeolites, the xylenes produced via toluene disproportionation comprise about 25% of the total xylenes obtained in the process.

Dealkylation of heavy reformate products containing ethyl groups can be traced by observance of the ethane yield. Thus, ZSM-5 and IM-5 zeolites exhibit the highest ethane yield, and this decreases with increasing pore size. Considering the total number of ethyl groups in the feed (ET, EX, and dEB ≈ 18.6 wt%), the maximum yield of ethane obtained by ethyl dealkylation is 4.4 wt%. Ethane yield is due principally to dealkylation reactions, but it can also be formed by cracking of naphthenes. Methane is produced in very low amounts ($< 0.3\%$) in all cases, showing that hydrogenolysis is occurring to a very low extent. The yields of cracking products (propane and butanes) do not show any clear dependence on zeolite structure, with beta the highest yield. It is worth noting that cracking products obtained with zeolite Y contained a significant amount of longer alkanes (pentanes and hexanes); these products were detected only in trace amounts in the rest of zeolites. This probably occurs because of the faster diffusion of longer chain hydrocarbons through the larger pore of Y zeolite, with the corresponding lower rate of re-cracking. Catalytic cracking of aromatics should require in a first step the hydrogenation of the aromatic ring over metallic clusters, producing naphthenes, which rapidly undergo cracking on the acid sites. Thus, cracking yield will depend not only on the zeolite structure, but also on the nature of the hydrogenating metallic particles, whose nature

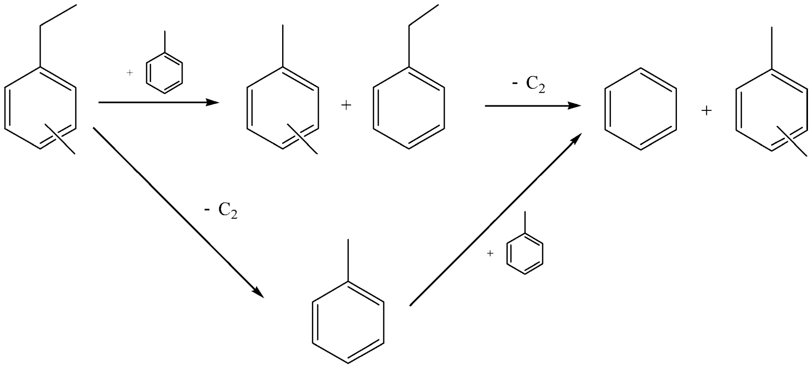

Scheme 1.

and size will be influenced by zeolite support properties like pore size, geometry, and acidity [20–22].

An important parameter in the catalytic evaluation of a transalkylation catalyst is the final content of ethylbenzene (EB) in the products, since the presence of EB in the *p*-xylene recovery unit strongly reduces the operating efficiency, and this can create a bottleneck in the production of xylenes in an industrial plant. The main reaction for the formation of EB from heavy reformate is the primary transfer of a methyl group from ethyltoluene to toluene (see Table 5), yielding one EB and one xylene molecule. Therefore, the EB formation should be lower with zeolites with high dealkylation activity and low transalkylation activity, that is, when the zeolite pore size is reduced. This dependence can be observed in Fig. 3A, which shows that ZSM-5 and IM-5 zeolites produce the lowest EB yield ($< 0.2\%$) and zeolite Y and beta produce the highest yields (1.8 and 1.2%, respectively) under the standard reaction conditions used here. Hence, it can be concluded that the best solution for reducing the final EB yield is to avoid transalkylation and to favor dealkylation from the beginning. This can be achieved with a catalyst that can induce the rapid dealkylation of the ethylaromatics (ET and EX), reducing in turn the ulterior undesired transalkylation of the methyl group from the ethyl toluene (see Scheme 1).

3.2.1. *Formation of heavy aromatics*

The formation of heavy aromatics (A_{10} and $A_{11}{}^{+}$) gives rise to progressive catalyst deactivation and reduces the selectivity of the process. Aromatics fraction A_{10}, composed principally of EX and TeMB, is produced in lower amounts over 10MR zeolites (see Fig. 3E), whereas the A_{10} yield increases with increasing zeolite pore size. This can easily be explained by a consideration of the steric impediments to the formation of EX and the different biphenylic transition states inside the pores of ZSM-5 and IM-5 and the high dealkylation activity shown by these zeolites.

The distribution of the different aromatics contained in the $A_{10}{}^{+}$ fraction is shown in the chromatogram of Fig. 5. It can be classified into three different groups: (i) naphthalene derivatives (methyl-, dimethyl-, trimethylnaphthalene) comprising up to 70% of the $A_{11}{}^{+}$ fraction; (ii) other polycyclic aromatics (PAH) like fluorenes, anthracenes, phenanthrenes, naphthacene, and pyrenes; and (iii) polyalkylbenzenes, including indanes, pentamethylbenzene, and ethylmethylbenzenes.

$A_{11}{}^{+}$ polyalkylbenzenes can be formed directly by transalkylation of A_9 molecules from the reformate feed [Eq. (1)]. Indeed, the primary products ethyltrimethylbenzene and diethylmethylbenzene can be produced by transalkylation of ET with TMB and by ET disproportionation

$$A_9 + A_9 \rightarrow A_7 + A_{11}. \tag{1}$$

As observed above for Re/beta catalyst, during the first contact of the fresh feed with the catalyst, $A_{11}{}^{+}$ is produced principally by ethyl transalkylation. This is due to the fact that the ethyl transalkylation rate is much higher than the dealkylation rate over large-pore zeolites [5]. These heavy products can further undergo ring closing and aromatization [23,24] to preferentially form naphthalene derivatives (see Scheme 2). This type of reaction is related to those occurring in reforming units at 440–500 °C, in which comparable hydrogen pressures and bifunctional catalysts like Al_2O_3–Cl/Pt–Re are used. The latter conversion of naphthalenic compounds to alkylbenzenes would involve hydrogenation and ring opening [25], but this reaction is not favored under the transalkylation process conditions, and their concentration increases, therefore, through the catalyst bed. From this we can conclude again that to avoid $A_{11}{}^{+}$ formation by transalkylation and the subsequent formation of very stable polycyclic aromatics, it is mandatory to dealkylate very rapidly the ethyl groups in the feed. It is clear that polycyclic aromatic compounds will occlude within the zeolite pore system, resulting in coke deposits and, therefore, in progressive catalyst deactivation. In addition, these molecules can give us an idea of the polynuclear aromatic (graphitic) nature of the coke deposited during the transalkylation process, in agreement with the results obtained by Magnoux et al. [26] during toluene disproportionation with H-USY zeolite. These authors found that the condensation degree of the aromatic rings contained in the coke increases with process temperature.

ITQ-23 has a unique structure that somehow promotes the formation of polycyclic aromatics (PAHs). The analysis

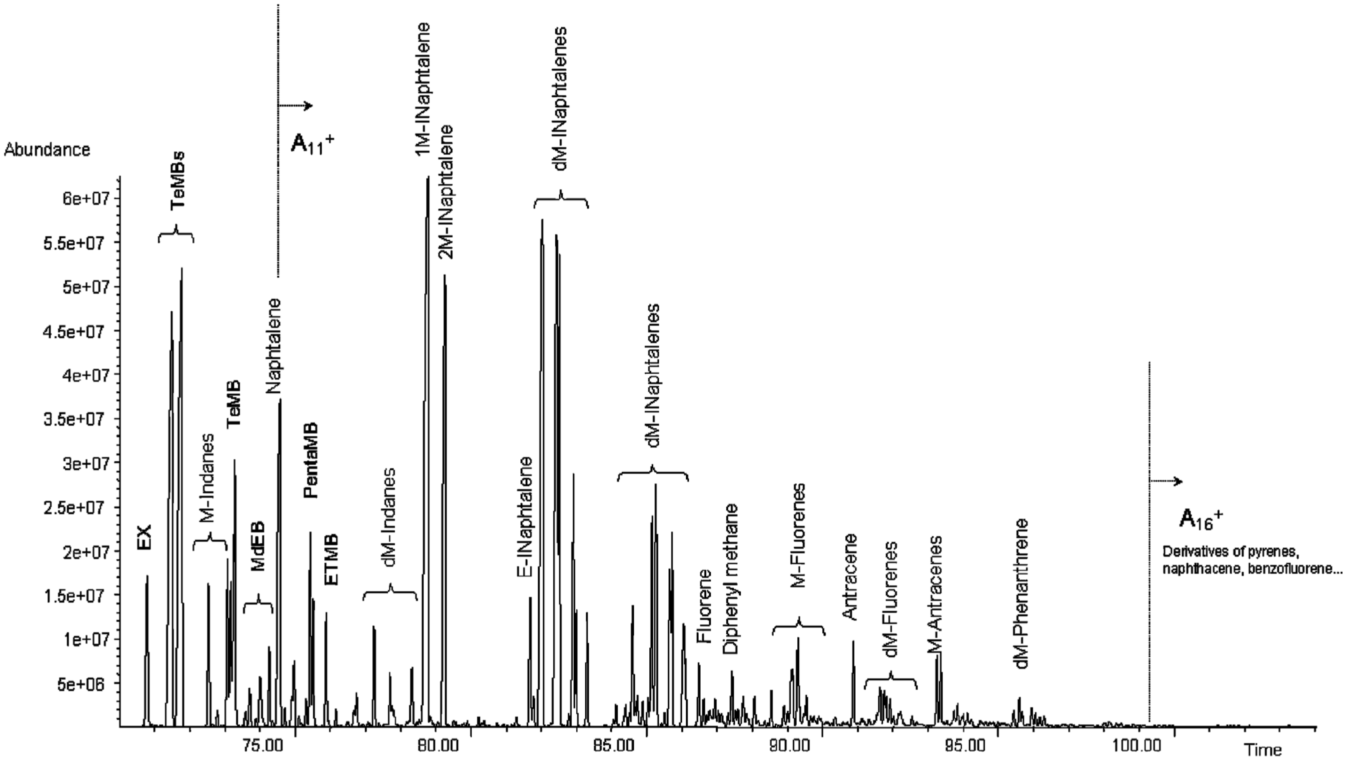

Fig. 5. GC-Analysis of the A_{11}^{+} fraction obtained by heavy reformate conversion over Re/ITQ-23 catalyst.

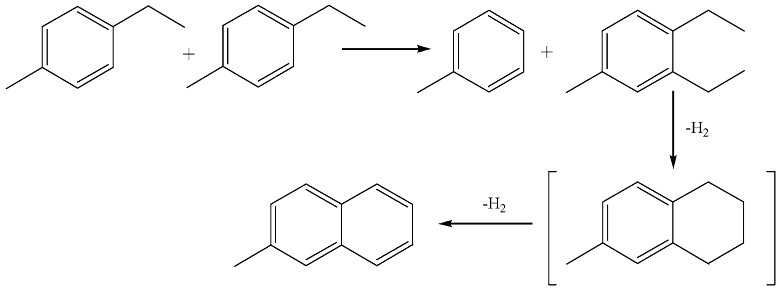

Scheme 2.

of this fraction obtained with the different zeolites showed that A_{11}^{+} distribution does not have a strong dependence on zeolite structure (Fig. 3E); it could be only said that the PAH percentage increases with decreasing pore size, which means with increasing dealkylation activity. Y zeolite produces a significant amount of very heavy aromatics (A_{16}^{+}) such as pyrene and its derivatives, whereas the amount of A_{16}^{+} produced by the rest of zeolites is almost undetectable.

3.2.2. Effect of contact time on zeolite selectivity

Fig. 6 shows the evolution of the yields of different products and conversion of TMB and ET with contact time for five different Re/zeolites. Zeolites NU-87 and ITQ-23 exhibit high xylenes and benzene yield (Figs. 6A–B) even for a contact time one-fourth as long as that in the standard test (WHSV $\approx 4\ h^{-1}$). The two zeolites also show a similar evolution for TMB and ET conversion and EB yield, whereas the A_{11}^{+} yield obtained with ITQ-23 is much higher than that obtained with NU-87. ZSM-5 shows a very high ET conversion at WHSV $\approx 16\ h^{-1}$ (Fig. 6D). Because of this very high dealkylation activity, this zeolite makes it possible to maintain EB and A_{11}^{+} yield at low levels even during the first steps of the reaction. The results at different contact times confirm and even make more clear the catalytic behavior observed for each zeolite at WHSV $\approx 4\ h^{-1}$.

The evolution of the yield of unstable poly-alkylbenzenes is similar for all five zeolites (Fig. 6F), that is, it increases rapidly at very low conversions and decreases at higher conversions. This behavior was previously observed for the conversion of pure EB over different zeolites [5], where unstable diethylbenzene was quickly formed by ethyl transalkylation and was subsequently converted by dealkylation at higher conversions (at higher contact times). With heavy reformate as the feed, polyalkylbenzenes formed by ethyl and propyl transalkylation are converted by dealkylation along the catalyst bed, but other A_{11}^{+} products like methyl-naphthalenes

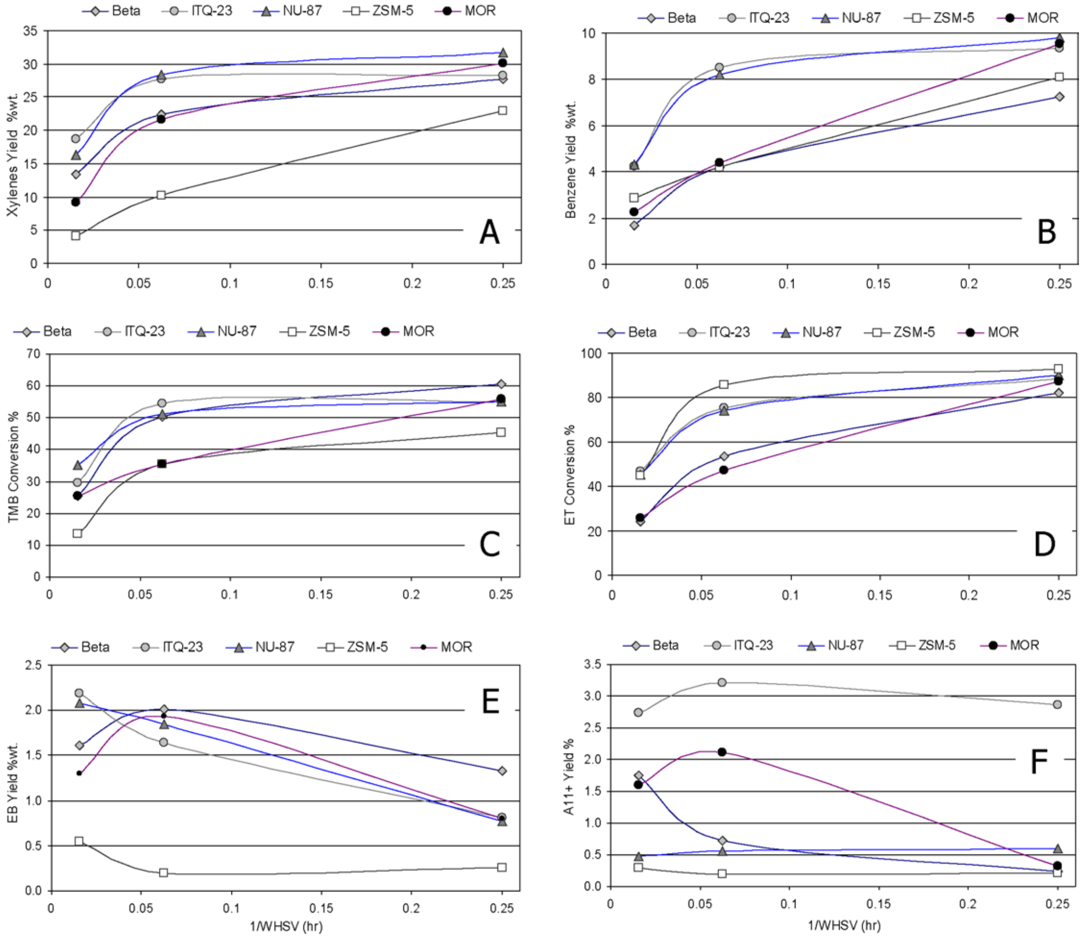

Fig. 6. Evolution of catalytic performance for four different Re/zeolite catalysts for a wide WHSV range (400 °C, $H_2/HC = 8.5$, and TOS ≈ 8 h).

are very stable and accumulate. This is especially visible in the case of ITQ-23 (Fig. 6F), for which the yield of $A_{11}{}^{+}$ reaches a maximum (∼ 3.3%) at WHSV ≈ 16 h^{-1} and decreases very little, even if the contact time is increased by a factor of 4.

Thus, in order to reduce the early formation of heavy products in the transalkylation unit, two different solutions can be adopted: (i) avoid their formation with an increase in shape-selectivity and external zeolite surface deactivation; and (ii) perform a fast dealkylation of ethyl and propyl groups contained in the A_9 feed, with an increase in the dealkylation activity of the catalyst. In addition, it is desirable for the catalyst to be able to dealkylate heavy polyalkylbenzenes, making it possible to convert the $A_{11}{}^{+}$ produced during the early steps of the process.

Tetramethylbenzenes (TeMBs) do not show the same behavior as that exhibited by $A_{11}{}^{+}$ products. For all zeolites, the TeMB yield increases for increasing contact time up to values close to the equilibrium, although medium-pore zeolites give some lower TeMB yield than the rest of the zeolite structures. Nevertheless, beta zeolite shows a slightly different evolution with contact time; that is, the TeMB yield reaches a maximum value for a short contact time and, after that, decreases up to values close to that obtained with the other zeolites. Indeed, the TeMB formation rate in zeolite beta should be much higher than that observed with the other studied zeolites, because of its tridirectional large pore system, which allows the diffusion of TMB and its disproportionation. Therefore, during the first steps of the reaction when TMB concentration is still very high, bimolecular TMB disproportionation is favored in beta zeolite, producing TeMB, which is subsequently converted mainly by transalkylation with toluene. Recently, the disproportionation of TMBs over large pore zeolites (mordenite, L zeolite, and beta) has been thoroughly studied [27], with special attention to the accessibility of the acid sites in the channel systems and the rate of transport of the bulky molecules involved.

Ethylbenzene is an unstable product that behaves similarly to $A_{11}{}^{+}$. Over all zeolites, a maximum yield of EB with contact time is observed, and the particular value is dependent on the zeolite structure. For instance, beta and ITQ-23 show a maximum yield of about 2% at WHSV ≈ 16 and 64 h^{-1}, respectively, whereas ZSM-5 shows a maximum yield of 0.6% at WHSV ≈ 64 h^{-1}. In the first reaction steps, ET is converted by dealkylation and transalkylation (specially with toluene; Scheme 1) to produce xylenes and EB as primary products. Subsequently, the EB produced is dealkylated along the catalyst bed. Consequently, highly dealkylating zeolites would reduce the final EB yield.

3.3. *Influence of the metallic function*

In this part of the work, the influence of the nature of the metal incorporated into the zeolite will be studied. Seven metals (Bi, Ga, La, Mo, Ni, Pt, Re) were impregnated into six different zeolites, and they were tested together with pristine H-zeolites for conversion of heavy reformate (Table 1). The aim of this part of the work was to study the effect of each metal on the activity and selectivity of each zeolite and to select the best one to be used in a finally optimized catalyst. Alario et al. [28] have shown that zeolites impregnated with $Ga(NO_3)_3$ by the procedure used in the present work give thin Ga platelets from 5 to 400 nm in average size. Hydrogen activation at 823 induces Ga migration into the zeolite micropores. In the case of our Ni- and Re-containing samples, TEM shows that the metals are formed of prismatic polydisperse particles embedded in the zeolite. Re appears to be more polydisperse (average size of 20 nm). An important fraction of the larger particles are on the zeolite surface. In the case of Ni, particles with a diameter of ~ 2 nm were also found.

Fig. 7 shows the yield of benzene and xylenes, the conversion of ET, and the yield of undesired products (EB, $A_{11}{}^{+}$, and cracking gases), with the 48 catalysts prepared. In general, the incorporation of the metal increases the yield of xylenes obtained with all zeolites, and the order is Mo $>$ Re $>$ Ni $>$ Ga $>$ Bi $>$ La $>$ Pt $>$ none. Re, Mo, Ni, and, to a smaller extent, Ga allow up to a 12% increase in the xylene yield, whereas Bi and La have little influence on the catalytic behavior of the zeolites. The incorporation of Pt produces an important increase in cracking yield (methane and C_3–C_4), because of the improved hydrogenolysis and aromatic ring hydrogenation activity of the Pt metallic clusters, which was rapidly followed by the acid cracking of the naphthenes over Brønsted acid sites to yield light paraffins. Even at 0.1 wt%, Pt shows a nonselective catalytic behavior that could be modified by treatments like sulfuration [9,34]. Saturates were detected in very low amounts ($< 0.2\%$) for all of the tested catalysts.

Re-, Mo-, and Pt-based catalysts show the highest dealkylation activity and achieve the highest ethyl- and propyl-aromatics conversion, and the highest ET dealkylation rates where obtained when they impregnated into ZSM-5 zeolite. Mo and Re incorporated into NU-87 and mordenite show the highest yield of xylenes and benzene, but also very high TMB conversion (transalkylation) and ET dealkylation. Bismuth impregnated into NU-87 and mordenite shows an unexpectedly high xylene yield together with a medium dealkylation activity. Ni-impregnated zeolites exhibit a high dealkylation activity, slightly lower than that shown by Re and Mo zeolites, and consequently they yield a higher amount of EB and $A_{11}{}^{+}$. In conclusion, the best performing metal-zeolite combinations are Re and Mo with mordenite and NU-87, with a high activity and a medium-high selectivity (low EB and $A_{11}{}^{+}$ Y), although the dealkylation activity and selectivity are still lower than those observed for (Re/Mo/Ga/Ni)-ZSM-5 catalysts.

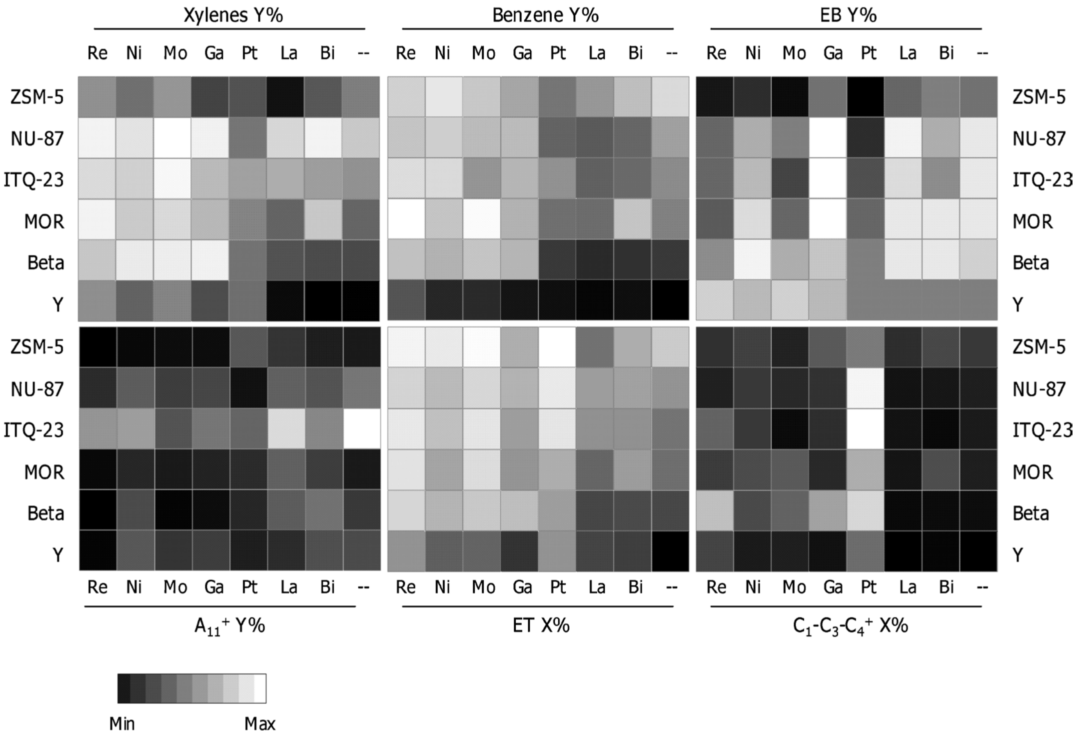

Fig. 7. Catalytic performance of metal-zeolite catalyst series (400 °C, WHSV 4 = h^{-1}, $H_2/HC = 8.5$, and TOS ≈ 8 h). Scale for each parameter (min–max): xylenes (13–31%), benzene (1–10%), EB (0–2.5%), $A_{11}{}^{+}$ (0–6%), ET (15–100%), C_1–C_3–C_4 (0.5–17%).

Table 6
Influence of Re content on Re-zeolite catalysts performance (400 °C, H_2/HC 8.5, and TOS ≈ 8 h; X (%) conversion and Y (wt%) yield)

Beta	WHSV 4 0% Re	WHSV 22[a] 0.3% Re[a]	WHSV 4 0.3% Re	WHSV 4 1.0 % Re
Xylenes *Y*	18.1	18.1	27.7	26.2
Benzene *Y*	3.2	3.0	7.3	6.4
Toluene *X*	36.5	22.3	37.5	44.6
TMB *X*	33.1	38.3	60.6	61.3
ET *X*	38.2	39.5	82.3	84.5
C3-B *X*	84.3	77.3	96.9	98.5
EX *X*	−22.4	−31.2	47.6	52.0
A_{10} *Y*	4.2	4.5	2.0	2.0
TeMB *Y*	1.15	1.20	0.98	0.92
$A_{11}{}^{+}$ *Y*	1.5	1.2	0.2	0.2
EB *Y*	1.9	1.8	1.3	1.1
CH_4 *Y*	0.01	0.01	0.2	3.5
Ethane *Y*	0.2	0.4	3.2	4.2
$C_3 + C_4{}^{+}$ *Y*	1.2	3.5	10.2	13.8

[a] Interpolated from experimental data.

Although Re produces a large improvement in the catalytic activity of zeolites, it has no apparent effect on the selectivity when compared at similar xylene yields (Table 6). The only differences in selectivity can be seen for $A_{11}{}^{+}$ yield, which is slightly higher for H-beta ($\Delta \approx 0.3\%$), whereas Re-beta (0.3%) shows a much higher yield ($\Delta \approx 2.3\%$) of cracking products (C_3–C_4), even when the contact time is about 5 times lower. Re incorporation strongly reduces the catalyst deactivation (see Fig. 8), since hydrogenating metallic clusters rapidly hydrogenate the olefins formed during dealkylation, therefore reducing the carbonaceous deposits formed by olefin polymerization and polyaromatics condensation. This effect is particularly visible for monodirectional 12MR zeolites like mordenite (Fig. 7). When the Re content is increased from 0.3 to 1 wt% over beta zeolite, there is a strong increase in cracking (C_3–C_4) and methane. Indeed, the samples containing 1 wt% Re are already able to hydrogenate aromatic rings, and the napthenes formed can crack on the acidic sites of the zeolite (Table 6).

3.4. Toward a rational design of the catalyst

Taking into account the process scheme established above and the behaviors of the different zeolites and metals, it is possible to design a transalkylation catalyst from *first principles*. Such a catalyst design would include the following functional components: (a) a highly active dealkylation function, to quickly remove the ethyl and propyl groups from reformate aromatics, and to dealkylate EB produced along the reactor bed; (b) a transalkylation function, responsible for the formation of xylenes and benzene; and (c) a selective hydrogenation function, to increase catalyst stability. From our previous study, we thought that a multizeolitic system that combines ZSM-5 and beta zeolite, together with Re as metal, should be a more appropriate catalyst than any of the single zeolite systems presented before in the literature.

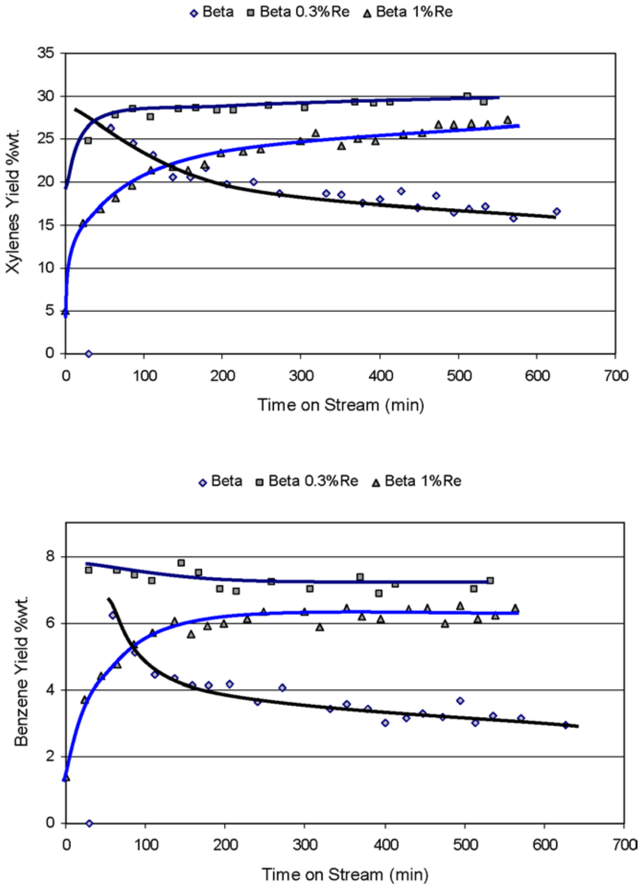

Fig. 8. Evolution with time on stream for the xylenes and benzene yield (wt%) for H-beta samples with different amounts of rhenium (400 °C, $H_2/HC = 8.5$, and WHSV = 4 h^{-1}).

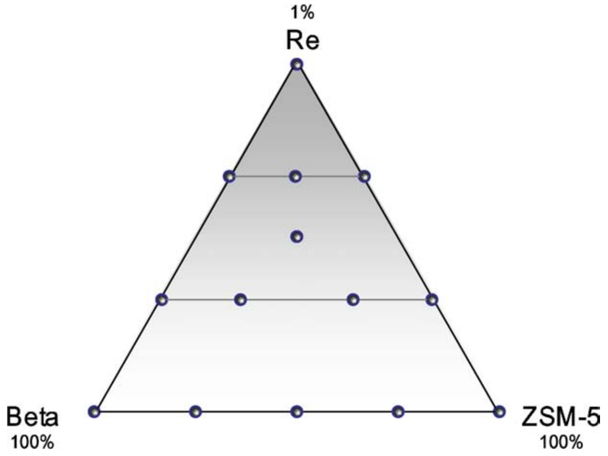

Fig. 9. Mixture design for the system ZSM-5/beta/rhenium.

Thus, we proceed to optimize the multizeolitic catalyst according to the experimental design shown in Fig. 9.

The different catalyst formulations were randomly synthesized and tested for reformate transalkylation, to avoid the effect of lurking variables. This experimental design makes it possible to obtain a general view of the influence of the different components on the catalyst performance and to iden-

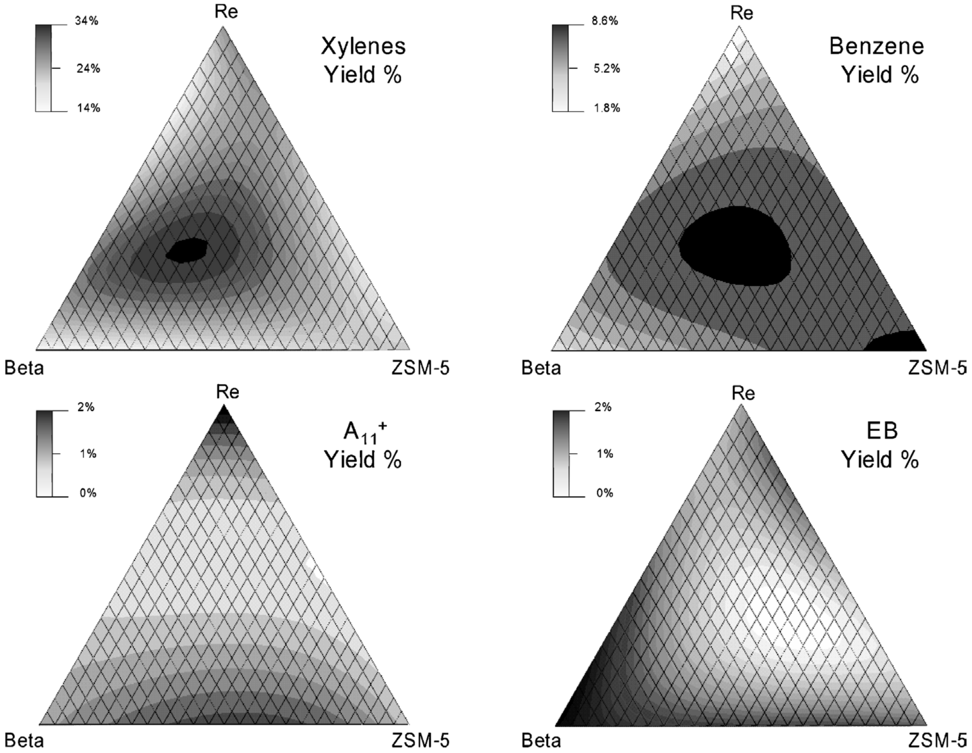

Fig. 10. Catalytic performance for the mixture design of the systems ZSM-5/beta/rhenium (400 °C, WHSV = 4 h^{-1}, H_2/HC = 8.5, and TOS ≈ 8 h).

tify nonlinear interactions (synergy) between components. Experimental results were fitted to a quadratic response surface, which will be employed as a prediction model for calculating/interpolating catalyst compositions with optimized features.

Fig. 10 shows the response surface of the yield of xylenes, benzene, $A_{11}{}^{+}$, and EB. Within the compositions considered in the design, a catalyst formulation (ZSM-5 40%, beta 60%, and Re 0.26%) was found to maximize the yield of xylenes (34%). This catalyst increases the best yield obtained with NU-87- or mordenite-based catalysts in the previous sections and with the best-performing heavy reformate dealkylation/transalkylation reference catalysts.

Regarding the formation of benzene, two catalyst compositions make it possible to maximize the benzene yield (∼ 8.4%); one is pure ZSM-5 zeolite, and the other is a mixed composition (around ZSM-5 50%, beta 50%, and Re 0.4%), which is very similar to that which maximizes the yields of xylenes. The EB yield is lower than 0.2% for ZSM-5-rich catalysts and for compositions located in the middle of the triangular design. For the catalyst composite giving the maximum xylene yield, the EB yield is still very low ($< 0.1\%$), especially when it is compared with the yield obtained with reference catalysts like Ni-mordenite (∼ 2.1) or Re-mordenite (∼ 0.8%). With respect to $A_{11}{}^{+}$, the lowest yields (0.5–0.8%) were obtained with Re- and ZSM-5-rich catalysts.

Additionally, the best composite catalyst found in this work can process reformate feeds with higher contents of A_9 and $A_{10}{}^{+}$, since the transalkylation (beta) and dealkylation (ZSM-5) components showed a high activity and stability, when tested for dealkylation of pure A_9 aromatics like *p*-ethyltoluene [5] and *n*-propylbenzene. Moreover, Re-beta component permitted dealkylation of heavy aromatics like EXs contained in $A_{10}{}^{+}$.

The combination of both Re/zeolites makes it possible to achieve much better results than those obtained by a consideration of the sum of their individual components. Indeed, taking into account the sum of the separated components (Re-ZSM-5 and Re-beta), the expected yield of $A_{10}{}^{+}$ and EB would be much higher, whereas the yield of xylenes would be much lower. Thus, we can say that a synergistic effect appears when the composite catalyst is used. This is mainly due to the improvement in the performance (activity and selectivity) of the beta zeolite due to the strong dealkylation activity of Re-ZSM-5, which rapidly reduces the content of ethyl- and propyl-aromatics. Furthermore, the reduction of the $A_{10}{}^{+}$ concentration in the gas stream makes it possible to improve the diffusion of lighter aromatics through the beta pore system, also increasing the concentration of the available toluene for the formation of xylenes by transalkylation with TMB. The blocking of the pore system due to the slow diffusion of $A_{10}{}^{+}$ molecules produces a reduction in the diffusion rate of the other aromatics like toluene and TMB, decreasing the global rate of the desired transalkylation reactions. Therefore, the addition of the dealkylation function increases the rate of formation of benzene and xylenes, but also the catalyst stability.

4. Conclusions

The reaction network for the dealkylation transalkylation process between commercial heavy reformate and toluene has been studied, and the influence of the zeolite structure and the nature of the metal incorporated into the yield of xylenes and benzene, the conversion of heavy reformate, and the yield of EB, heavy aromatics A_{11}^{+}, and cracking products has been determined. It is concluded that medium-pore zeolites (ZSM-5) impregnated with Mo or Re give high dealkylation activity of the ethyl- and propyl-aromatics contained in heavy reformate, but show moderate TMB conversion and xylene yield. A valuable aspect of these catalysts is the production of low levels of undesired products like EB and A_{10}^{+}. These have been found to be formed in the first reaction steps when the rate of transalkylation with respect to dealkylation, particularly for ethyl and propyl groups, becomes higher.

Large-pore zeolites show high activity for transalkylation, which favors the desired TMB conversion, and the formation of xylenes. However, their dealkylation activity for propyl- and ethyl-aromatics is low. Zeolites with intercrossing channels of 12MR + 10MR and 12MR + 8MR, impregnated with Re, Mo, Ni, and Bi, combine high dealkylation and transalkylation activities, resulting in high yields of xylenes. The only drawback of these catalysts is the still too high yield of undesired products (EB and A_{10}^{+}) and the possible deactivation problems.

A rational catalyst design has been carried out in this work, which involves a selective multizeolitic catalyst. This makes it possible to combine a very active transalkylation function for producing xylenes (beta, NU-87, or MOR impregnated with Mo/Re/Bi), together with a highly enhanced dealkylation function (ZSM-5 impregnated with Mo/Re). This dealkylation function removes the ethyl and propyl groups very quickly from heavy reformate compounds, increasing the final performance of transalkylation function because of the following facts: (i) a larger amount of toluene and benzene is available for transalkylation with TMB and TeMB; (ii) a lower amount of EB and heavy aromatics is produced, increasing the selectivity; and (iii) catalyst life is improved because of the formation of a lower amount of A_{11}^{+}.

Acknowledgments

The authors thank the Institut Français du Pétrole and Comisión Interministerial de Ciencia y Tecnología (CICYT) (Project MAT 2003-07945-C02-01) for financial support and S. Leiva for help with the zeolite preparation.

References

[1] T.-C. Tsai, S.-B. Liu, I. Wang, Appl. Catal. A 181 (1999) 355.
[2] S.H. Oh, S.I. Lee, K.H. Seong, Y.S. Seong, Y.S. Kim, J.H. Lee, Upgrading of reformate and heavy aromatics to high-value BTX, in: 2nd Asian Petrochem. Tech. Conference APTC 2002, Seoul, Korea, 7–8 May 2002.
[3] J.R. Mowry, R.A. Meyers (Eds.), Handbook of Petroleum Refining Processes, McGraw–Hill, New York, 1986, Section 10-10.
[4] Mobil Transplus Brochure, Mobil Technology Company.
[5] J.M. Serra, E. Guillon, A. Corma, J. Catal. 227 (2004) 459.
[6] J. Čejka, B. Wichterlová, Catal. Rev. 44 (2002) 375.
[7] G.A. Olah, A. Molnar, Hydrocarbon Chemistry, Wiley, New York, 1995.
[8] M. Guisnet, N.S. Gnep, S. Morin, Micropor. Mesopor. Mater. 35–36 (2000) 47.
[9] T. Tsai, W.-H. Chen, S.-B. Liu, C.-H. Tsai, I. Wang, Catal. Today 73 (2002) 39.
[10] A.V. Sapre, B.C. Gates, Ind. Eng. Chem. Process. Des. Dev. 21 (1982) 86.
[11] A. Stanislaus, B.H. Cooper, Catal. Rev. 36 (1994) 75.
[12] M.D. Shanon, J.L. Casci, P.A. Cow, S.J. Andrews, Nature 353 (1991) 417.
[13] A. Corma, A. Chica, J.M. Guil, F.J. Llopis, G. Mabilon, A. Perdigón-Melón, S. Valencia, J. Catal. 189 (2000) 382.
[14] C.J. Kuei, L.J. Leu, Zeolites 9 (1989) 193.
[15] A. Corma, I. Giménez, S. Leiva, F. Rey, M.J. Sabater, G. Sastre, S. Valencia, in: Proceedings of 14th Int. Zeol. Conf., Cape Town, South Africa, 25–30 April 2004.
[16] C.A. Emeis, J. Catal. 141 (1993) 347.
[17] J.H. De Boer, B.C. Lippens, B.G. Linsen, J.C.P. Broekhoff, A. van den Heavel, Th.V. Osinga, J. Colloid Interface Sci. 21 (1996) 405.
[18] A. Corma, J.M. Serra, A. Chica, in: E.G. Derouane, V. Parmon, F. Lemos, F. Ramôa Ribeiro (Eds.), Principles and Methods for Accelerated Catalyst Design and Testing, Kluwer-Academic Publishers, Dordrecht, 2002, p. 153.
[19] A.Corma, J. Hernández, J.M. Serra, World Patent WO0159463 (2001), to CSIC-UPV.
[20] A. Corma, A. Martínez, V. Martínez-Soria, J. Catal. 169 (1997) 480.
[21] P. Gallezot, G. Bergeret, in: E.E. Paersen, A.T. Bell (Eds.), Catalysis Deactivation, Dekker, New York, 1987, p. 129.
[22] W.M.H. Sachtler, Z. Zhang, Adv. Catal. 39 (1993) 129.
[23] S.G. Brandenberger, W.L. Callender, W.K. Meerbott, J. Catal. 42 (1976) 282.
[24] B.H. Davis, Catal. Today 53 (1999) 443.
[25] M.A. Arribas, A. Martínez, Appl. Catal. 230 (2002) 203.
[26] P. Magnoux, C. Canaf, F. Machado, M. Guisnet, J. Catal. 134 (1992) 286.
[27] J. Čejka, J. Kotrla, A. Krejčí, Appl. Catal. A 277 (2004) 191.
[28] J.F. Joly, H. Ajot, E. Merlen, F. Raazt, F. Alario, Appl. Catal. A 79 (1991) 249.
[29] A.B. Halgeri, J. Das, Appl. Catal. 181 (1999) 347.
[30] G. Nacamuli, R. Vogel, S. Zones, US Patent 5952536 (1999), to Chevron Chem.
[31] F. Alario, E. Benazzi, US Patent 6,037,512 (2000), to IFP.
[32] F. Raatz, P. Dufresne, C. Marcilly, US Patent 4,723,048 (1998), to IFP.
[33] A. Ghosh US Patent 6,096,938 (2000), to Fina Teck.
[34] O. Martin, A. Alario, N. Ferrer, E. Merlen, Eur. Patent 1,077,083 (2003), to IFP.
[35] I. Kazuyosi, I. Ryoji, K. Jaime, T. Hitoshi, Eur. Patent EP0816311 (1998), to Toray Industries.
[36] F. Alario, E. Merlen, US Patent 6,486,372 (2002), to IFP.
[37] C. Drake, A.-H. Wu, US Patent 6,017,840 (2000), to Phillips Petroleum.
[38] C. Drake, A.-H. Wu, US Patent 5,866,741 (1999), to Phillips Petroleum.
[39] J.P. Verduijn, G.D. Mohr, US Patent 6,008,425 (1999), to Exxon Chem.
[40] W. Cheng, D. Kong, D. Yang, H. Li, Z. Zhu, US Patent 6,500,997 (2002), to China Petro-Chemical Corporation.
[41] R. Icioka, H. Okino, S. Yamakawa, US Patent 5,847,256 (1991), to Toray Ind.